Heat Fluxes Localization and Abnormal Size Effect Induced by Multi-Body Vibration in Complex Networks

Kezhao Xiong (xiongkezhao@outlook.com)
Xi'an University of Science and Technology
Zhengxin Yan
Xi'an University of Science and Technology
You Xie
Xi'an University of Science and Technology
Yixian Wang
Xi'an University of Finance and Economics
Chunhua Zeng
Kunming University of Science and Technology
Zonghua Liu
East China Normal University

Research Article

Keywords: Multibody dynamics, Complex networks, Heat conduction

Posted Date: November 15th, 2021

DOI: https://doi.org/10.21203/rs.3.rs-935085/v1

Nonlinear Dynamics manuscript No.
(will be inserted by the editor)

Heat fluxes localization and abnormal size effect induced by multi-body vibration in complex networks

Kezhao Xiong · Zhengxin Yan · You Xie · Yixian Wang · Chunhua Zeng · Zonghua Liu

Received: date / Accepted: date

Abstract Heat conduction in real physical networks such as nanotube/nanowire networks has been attracting more and more attention, but its theoretical understanding is far behind. To open a way to this problem, we present a multi-body vibration model of heat conduction to study how heat is conducted in complex networks, where nodes' degrees satisfy a random distribution and links consist of 1D atom chains with nonlinear springs. Based on this model, we find two interesting phenomenons: (1) The main heat fluxes of network are always localized in a skeleton subnetwork, which may have potential applications in thermal management and thermal concentrators, etc; (2) There exists an abnormal size effect of heat conduction in complex networks, i.e. the total heat flux of network will be enlarged with the increase of atoms on links, which is in contrast to the previous result on a 1D chain. Furthermore, we introduce a transmission diagram to characterize the skeleton of localized heat fluxes and then discover a phase transition of total heat flux in the process of removing links, implying that the control of heat flux can be effective only when the change of network topology is focused on the links within the skeleton. A brief theory is introduced to explain the abnormal size effect.

Keywords Multibody dynamics · Complex networks · Heat conduction

K. Xiong (✉) · Z. Yan · Y. Xie · Y. Wang
College of Science, Xi'an University of Science and Technology, Xi'an 710054, P.R. China
E-mail: xiongkezhao@outlook.com

C. Zeng
Institute of Physical and Engineering Science, Kunming University of Science and Technology, Kunming 650500, P.R. China

Z. Liu
School of Physics and Electronic Science, East China Normal University, Shanghai, 200062, P. R. China

1 Introduction

Complex networks are ubiquitous in both natural and artificial systems and have been well studied in last two decades [1–3]. It is revealed that most of complex networks have the features of small world and heterogeneity, which are the basis for tremendous applications such as in the aspects of communication in internet, synchronization in brain, and epidemic spreading in social networks [4–8] etc. However, little attention has been paid to the aspect of heat conduction in complex networks, except a few works [9–15]. In fact, this problem is becoming more and more important, due to the fast developing of massive integration methods boost the interconnected intact structure of the nano-network extending from microscale to macroscale, and provide practical applicability in device designs [16, 17]. On the other hand, more and more experiments on nano-networks have demonstrated remarkable properties for many applications, such as nano-filtration [18], energy storage [19], electronic skin [20], sensors [21], neuromorphic networks [22], thermal management [23], optical elements [24], electrocatalysis [25] etc. A characteristic feature of these real networks is that their individual links can be considered as 1D atoms chains [13], implying that the knowledge obtained in 1D and 2D lattices [26–28] will be helpful for us to study heat conduction in nano-networks.

A distinctive difference between complex networks and 1D/2D lattices is that the degrees of nodes are distributed in a range for the former but the same for the latter. This difference will make their heat conduction be fundamentally different. For example, it was shown by an oversimplified network model that the network topology can seriously influence its heat conduction and result in a rectification effect [9], positive degree correlation (assortativity) can enhance thermal transport but negative degree correlation (disassortativity) can weaken it [12], interface thermal

resistance exists at all the nodes of complex network and their values depend sensitively on the sites of nodes and the coupling strengths of connected links, which make the theoretical analysis of heat conduction in complex networks be a challenge problem [11, 29]. In addition, it was shown that the heat flux can go from a low-temperature node to a higher-temperature node, and there exits an optimal network structure that displays small thermal conductance and large electrical conductance [14].

However, realistic nanotube/nanowire networks are much complicated than the oversimplified network model. Take the links as an example, the former can be considered as 1D atoms chains [13], while the latter are only simplified as springs. Then, an interesting but challenging problem is how the interaction of different 1D atoms chains at each individual node influences the heat conduction on the whole network. To solve this problem, we here present a multi-body vibration model of heat conduction where nodes' degrees satisfy a random distribution and links consist of 1D atom chains with nonlinear springs, as shown in Fig. 1.

The remainder of the paper is organized as follows. In Sec. 2, we present a random network to represent the nanotube and nanowire networks, where links are 1D atom chains and their motion satisfies the canonical equations. In Sec. 3, we do a lot of numerical simulations and unfold some fascinating phenomenons including the localization of heat fluxes, jumping transition of total heat flux in the process of removing links, and skeleton subnetwork of heat conduction in networks. Moreover, an abnormal size effect of heat conduction in physical networks is revealed, i.e. the total heat flux increases with the increase of links length, in contrast to the case of 1D chain. In Sec. 4, a brief theory analysis referring to interface thermal resistances is introduced to explain the abnormal size effect. Conclusion and discussion are presented in Sec. 5.

2 The model

The multi-body vibration model of heat conduction on physical networks can be shown by the schematic Fig. 1, where the the "green" points represent the nodes and the "blue" points denote the atoms on links, the nodes with the "red" and "black" circles contact heat baths with high temperature T_h and low temperature T_ℓ respectively, and n_{ij} represents the amount of atoms on the link ℓ_{ij} connecting the two nodes i and j. It is clear that each atom on a link is connected only to its two nearest neighbors while the atom at node-i is connected to its k_i nearest neighbors. To study heat conduction of this model, we first construct a random network by the approach in Ref. [1] with size N and average degree $\langle k\rangle$. Then, we put atoms on the network, represented by all the points in Fig. 1. We assume n_{ij} to be a random number from a uniform distribution and satisfies $n_1 \le n_{ij} \le n_2$,

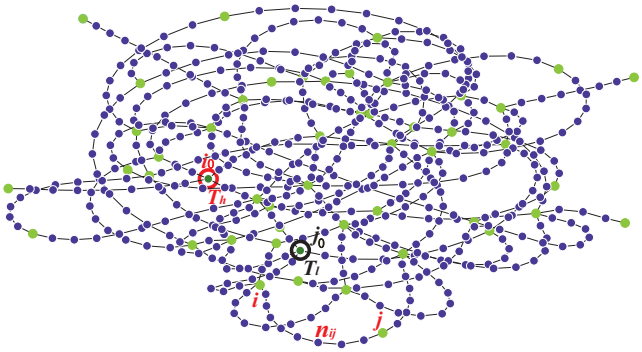

Fig. 1 (color online). Schematic figure of a physical network, where the "green" points represent the nodes, the "blue" points denote the atoms on links, i_0 and j_0 represent two heat source nodes contacting the two thermostats with the low temperature T_ℓ and high temperature T_h respectively, and n_{ij} represents the amount of atoms on link-ℓ_{ij} between the two connected nodes i and j.

i.e. $n_{ij} = n_1 + (n_2 - n_1 + 1) \times rand$. We here set $n_1 = 3$ and $n_2 = 11$, if without specific illustration. Following Ref. [30], we make both the nodes and the atoms on links be the same FPU-β oscillator with Hamiltonian

$$H = \sum_i \left[\frac{1}{2}p_i^2 + V_i(x_i)\right], \tag{1}$$

for the atoms on a link ℓ_{ij} with amount n_{ij}, they have a potential

$$V_i(x_i, x_{i+1}) = \frac{C_{i,i+1}}{2}\left[(x_{i+1} - x_i)^2 + \frac{g_4}{2}(x_{i+1} - x_i)^4\right], \tag{2}$$

for the atoms at nodes, their potential satisfy

$$V_i(x_i, x_j) = \frac{1}{2}\sum_{j=1}^{k_i} C_{i,j}\left[\frac{1}{2}(x_i - x_j)^2 + \frac{g_4}{4}(x_i - x_j)^4\right], \tag{3}$$

where x_i represents the displacement from the equilibrium position of the i-th atom, $C_{i,j}$ is the coupling strength between the node i and its neighboring atom j, $C_{i,i+1}$ is the coupling strength between two neighboring atoms i and $i+1$ on a link and equal to $C_{i,j}$ for the same link, k_i is the number of links connecting the i-th atom, the sum is for all the nearest neighboring atoms j of node-i, and g_4 is the normalized nonlinear constant, which is 0.1 in this paper. In our simulations, fixed boundary conditions for two nodes i_0 and j_0 that attached to the two heat bathes are used. The heat bath is stochastic Langevin heat bath and the coupling strength determined by the friction coefficient γ in Langevin dynamics is 5 in this paper. This value is within the range of $\gamma \in (1, 100)$ that recommended by Chen et al [31] so that a meaningful physics can be obtained.

The motion of all nodes and atoms satisfies the canonical equations

$$\frac{dp_i}{dt} = -\frac{\partial H}{\partial x_i}. \tag{4}$$

To discuss heat conduction on the constructed network, we randomly choose two nodes i_0 and j_0 as the source nodes to

contact two heat baths with temperature T_h and T_ℓ, respectively (see Fig. 1). Therefore, they satisfy

$$\frac{dp_h}{dt} = -\frac{\partial H}{\partial x_h} + \Gamma_h - \gamma p_h, \tag{5}$$

$$\frac{dp_l}{dt} = -\frac{\partial H}{\partial x_l} + \Gamma_l - \gamma p_l, \tag{6}$$

where $\Gamma_{h,l}$ are the Gaussian white noises with

$$\langle \Gamma_{h,l}(t) \rangle = 0, \tag{7}$$

$$\langle \Gamma_h(t)\Gamma_h(0) \rangle = 2\gamma k_B T_h \delta(t), \tag{8}$$

$$\langle \Gamma_l(t)\Gamma_l(0) \rangle = 2\gamma k_B T_l \delta(t), \tag{9}$$

where k_B is the Boltzmann constant, and we adopt the dimensionless unit by setting $k_B = 1$.

As $T_h > T_\ell$, there will be heat fluxes continuously pumped from node i_0 to node j_0 through other nodes and links in the network. Specifically, the heat fluxes will be firstly transmitted from node-i_0 to other nodes through all the links of node-i_0, and then gradually merge and finally go to node-j_0 through the links of node-j_0. After the transient process, the network will reach a stationary state. The local temperature at each atom i can be defined as [26, 27]

$$T_i = \langle p_i^2 \rangle, \tag{10}$$

and the local flux J_{ij} on each link-ℓ_{ij} can be calculated by [26, 32–34]

$$J_{ij} = \langle \dot{x}_i \frac{\partial V}{\partial x_{i+1}} \rangle, \tag{11}$$

where $\langle \cdots \rangle$ is the time average.

3 Numerical simulations

3.1 Heat fluxes localization

In numerical simulations, we set the network size $N = 50$ and average degree $\langle k \rangle = 4$, randomly choose two nodes as the source nodes-i_0 and j_0 respectively, and let $T_h = 1$ and $T_\ell = 0.1$ in this work. Then, We calculate the heat fluxes J_{ij} for all the links in the network by Eq. 11, and schematically illustrate transmission diagram of heat fluxes in Fig. 2(a). For clarity, we only plot all the nodes and their links in Fig. 2(a) but do not show the atoms on all links, where the arrows denote the directions of the fluxes J_{ij}, the widths of arrows denote the values of heat fluxes J_{ij}, and the wider of the width, the greater of the value. From Fig. 2(a) we see clearly that some links have larger fluxes while other links have smaller fluxes and even approximately zero flux, which means different links on the network have different effects on heat conduction. In order to further understand the influence of different links on heat conduction, one of the richest tools is removing links [35]. Hence, we probe the influence

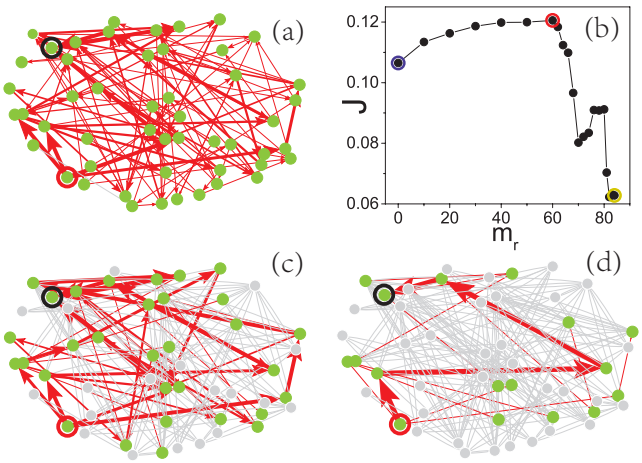

Fig. 2 (color online). (a) Transmission diagram of heat fluxes on a random network, where the arrows denote the directions of the fluxes J_{ij} on link-ℓ_{ij}, the widths of arrows denote the values of heat fluxes J_{ij}, the network size $N = 50$ and average degree $\langle k \rangle = 4$, and two nodes in red and black circles are randomly chosen as the source nodes-i_0 and j_0 contacting with $T_h = 1$ and $T_\ell = 0.1$, respectively. (b) The change of total heat flux J with the amount of removing links m_r, where the points in bule, red and yellow circles are corresponding to the cases of Fig. 2(a), (c) and (d), respectively. (c) and (d) are the transmission diagrams of heat fluxes for the remaining structure after greying the removed 60 and 84 links, corresponding to the point with red and yellow circles in Fig. 2(b).

of removing links in the network on the total heat flux J of the network, which is the sum on all the paths from the high temperature source node-i_0 to its neighbors or the sum on all the paths to the low temperature source node-j_0. Taking the network corresponding to Fig. 2(a) as an example, without any change of other parameters, we remove the links in the network one by one according to the order of its heat flux value from small to large, and present the dependence of total heat flux J on the amount of removing links m_r, as shown in Fig. 2(b). We can see clearly that the total heat flux J will gradually increase to a optimal value with the increase of m_r at first, but surprisingly appear a sharp jump after m_r increase to 60. According to the parameters of the generated network corresponding to Fig. 2(a), we know only 40 links are remained after removing 60 links. The sharp jump in Fig. 2(b) indicates the remaining 40 links are crucial to network heat conduction. On the other hand, according to the order of removing links, the heat flux values of the remaining 40 links are larger than the removed 60 links. After calculation, the sum of heat flux values of the remaining 40 links can approximately account for 70 percent of the sum of heat flux values of all links in the network. This means heat fluxes are localized and controlled by these remaining 40 links, therefor we call it *skeleton subnetwork*.

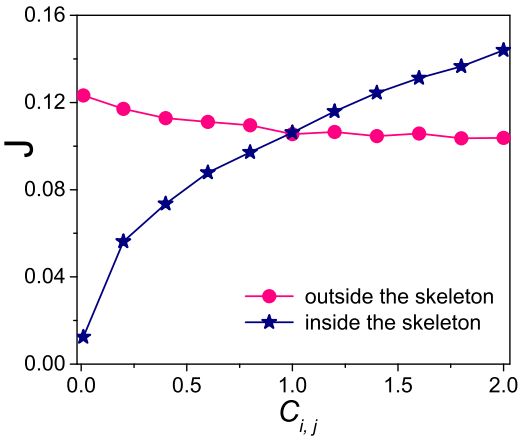

Fig. 3 (color online). The dependence of the total heat flux J in the network on the coupling strength $C_{i,j}$, where the blue stars are corresponding to the situations of just regulating coupling strength $C_{i,j}$ inside the *skeleton subnetwork* but maintain $C_{i,j}$ outside the *skeleton subnetwork* as the constant value 1, on the contrary, the solid pink circles are corresponding to the situations of just regulating coupling strength $C_{i,j}$ outside the *skeleton subnetwork* but maintain $C_{i,j}$ inside the *skeleton subnetwork* as the constant value 1.

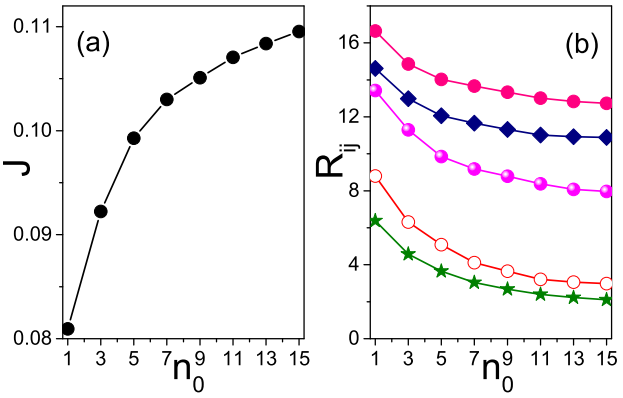

Fig. 4 (color online). Abnormal size effect on network. (a) The dependence of total heat fluxes J on atoms amount n_0, where $n_1 = n_2 = n_0$ and the other parameters are the same as the network in Fig. 2(a). (b) Dependence of the thermal resistances $R_{ij} = |T_i - T_j|/J_{ij}$ on n_0 for 5 links randomly chosen from the network correspond to Fig. 4(a).

For visualization of the *skeleton subnetwork*, we schematically illustrate the transmission diagram of heat fluxes after graying the removed 60 links, i.e. the remaining structure corresponding to the point in a red circle in Fig. 2(b), as shown in Fig. 2(c). Moreover, we further illustrate the heat flux diagram when $m_r = 84$, i.e. the remaining structure corresponding to the point with a yellow circle in Fig. 2(b), as shown in Fig. 2(d). From Fig. 2(d), we can clearly see that after the removed 84 links are grayed out, only one heat conduction path remains from the high temperature source node in the red circle to the low temperature source node in the black circle, which means $m_r = 84$ is the maximum amount of removed links that the network can endure, and leads to the minimum total heat flux J in Fig. 2(b).

In order to further understand the influence of *skeleton subnetwork* on network heat conduction, we regulate the coupling strength $C_{i,j}$ of Eq. 3 inside and outside the skeleton, respectively. Firstly, we maintain the coupling strength of the part outside the *skeleton subnetwork* as the constant value 1, just regulate the coupling strength $C_{i,j}$ inside the *skeleton subnetwork*, and present the dependence of the total heat flux J in the network on the coupling strength $C_{i,j}$, as shown by the blue stars in Fig. 3. Then, on the contrary, we maintain the coupling strength of the part inside the *skeleton subnetwork* as the same value 1, just regulate the coupling strength $C_{i,j}$ outside the *skeleton subnetwork*, and present the dependence of the total heat flux J in the network on the coupling strength $C_{i,j}$, as shown by the solid pink circles in Fig. 3. We interestingly find that the total heat flux J will monotonically increase with the increase of coupling strength $C_{i,j}$ inside the *skeleton subnetwork*, while weakly decrease with the increase of coupling strength $C_{i,j}$ outside the *skeleton subnetwork*, indicating that the heat conduction in the original network can be approximately replaced by that in the *skeleton subnetwork*. We have checked a variety of other networks and confirmed that the localization of heat fluxes and the jumping transition are general phenomenon in physical networks. Thus, the total heat flux of network is keen to the varying of network topology only when the change happens in the skeleton subnetwork but not keen otherwise, implying that the control of heat flux will be effective only when the controlled links are chosen from the skeleton subnetwork. In this sense, maybe we can make the heat fluxes of networks be pumped into the skeleton from outside the skeleton by the way of regulating the coupling strength inside the skeleton subnetwork, implying potential applications in controlling heat diffusion and thermal concentrators [37, 38].

3.2 Abnormal size effect

Now, we turn to the size effect of n_{ij}. For this purpose, we consider a specific situation with $n_1 = n_2 = n_0 - 2$ and focus on the dependence of total heat flux J on n_0, where the other parameters are same to the network in Fig. 2(a). Fig. 4(a) shows the dependence of total heat flux J on n_0, where we can see that J increase monotonically with n_0, in contrast to the 1D case where J decreases with the increase of system size [26–28], indicating an *abnormal size effect*. To figure out the answer, we randomly choose 5 links ℓ_{ij} from the network correspond to Fig. 4(a) and calculate their thermal resistances $R_{ij} = |T_i - T_j|/J_{ij}$ under different link length n_{ij}, as shown in Fig. 4(b). We see that thermal resistance R_{ij} de-

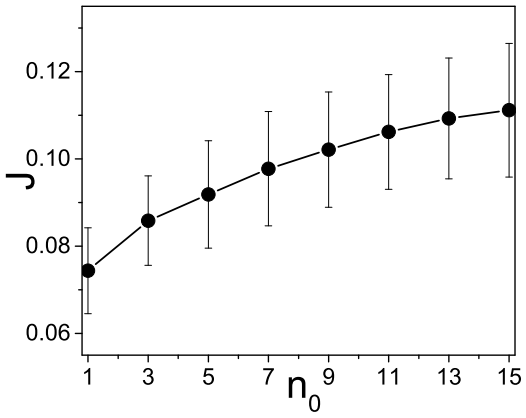

Fig. 5 (color online). The dependence of total heat fluxes J on atoms amount n_0, where J is an average on 50 randomly generated networks with size $N = 50$, average degree $\langle k\rangle = 4$, and the the coupling strength $C_{i,j} = 1.0$.

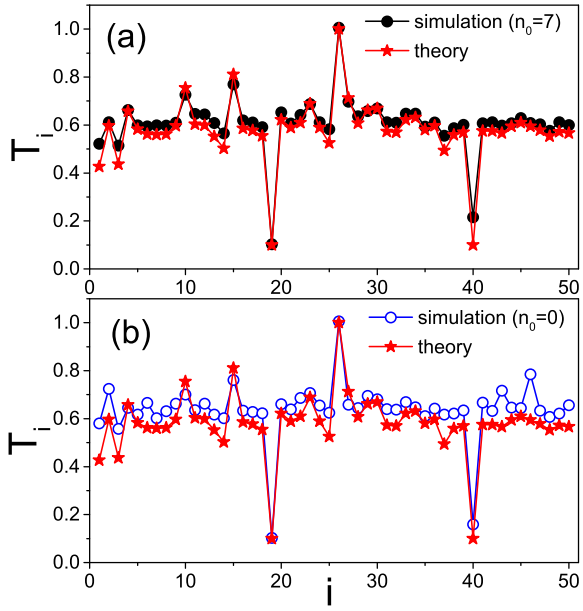

Fig. 6 (color online). Temperature distribution comes from numerical simulation and theory. (a) The comparison between the simulation result for the case of $n_0 = 7$ and the theoretical result by Eq. (13). (b) The comparison between the simulation result for the case of $n_0 = 0$ and the theoretical result by Eq. (13).

crease monotonically with increase of n_0, which means the total thermal resistance of a network will be weaken by increasing atoms, thus make total heat flux J increase with n_0. We have checked a variety of network topologies and confirm that the *abnormal size effect* is a general phenomenon in physical networks, as shown in Fig. 5. Specifically, for each n_0 in Fig. 5, the total heat flux J is an average on 50 randomly generated networks with size $N = 50$, average degree $\langle k\rangle = 4$, and the coupling strength $C_{i,j} = 1.0$.

In order to better understand this phenomenon, a few more words should be given to the effect of interface thermal resistance. For fixed temperature of Langevin heat bath, J is determined by the thermal resistance of links in a network. For each link ℓ_{ij}, there is always interface thermal resistances at its two ends [29]. With the increase of n_0 from 1 to 15, the added new atoms will significantly decrease the interface thermal resistances thus cause the decrease of R_{ij} and the *abnormal size effect*, which will be confirmed later by theoretical analysis.

4 Theoretical analysis

Actually, the existence of interface thermal resistances make the theoretical derivation of heat conduction on complex networks be a big challenge [9]. However, it is maybe possible to make a brief theoretical derivation for the influence of network topology on heat conduction when the interface thermal resistances is ignored. In this situation, we ignore all the information on the detailed dynamics of atoms, but only concern how the temperatures and heat fluxes are distributed on a network based on topological structure of a given network and two chosen source nodes. Thus, the physical network of Fig. 1 can be simplified as a matrix $A = (a_{ij})$ with $a_{ij} = 1$ if i and j are connected and 0 otherwise. Specifically, we let $a_{ii} = 0$. Making a transformation of A, we have $L = I - D^{-1}A$ with I being the identity matrix and D being the diagonal degree matrix. We let $\mathbf{M}$ be the temperature vector of N nodes. For convenience, we reorganize the network and let the source nodes with T_h and T_ℓ be the nodes 1 and 2, respectively, which results in $\mathbf{M} = (T_h, T_\ell, T_3, \cdots, T_N)^T$. $\mathbf{M}$ can be divided into two blocks with block-1 $\mathbf{M}_1 = (T_h, T_\ell)^T$ and block-2 $\mathbf{M}_2 = (T_3, \cdots, T_N)^T$.

Applying the Fourier's law $J = -\kappa\nabla T$ to network, we have $\mathbf{J}(\mathbf{r}) = -\kappa\nabla\mathbf{M}(\mathbf{r})$. Further, we obtain

$$\nabla\cdot\mathbf{J}(\mathbf{r}) = -\kappa\nabla^2\mathbf{M}(\mathbf{r}). \tag{12}$$

The discrete Laplace operator L can be considered as an analog of $-\nabla^2$ [36]. Substituting it into Eq. (12), we have $\mathbf{LH} = \mathbf{f}$ where $H(i)$ plays the role of $\kappa\mathbf{M}(\mathbf{r})$ and $f(i)$ plays the role of $\nabla\cdot\mathbf{J}(\mathbf{r})$. Corresponding to $\mathbf{M}_1$ and $\mathbf{M}_2$, $\mathbf{H}$ can be divided into $\mathbf{H}_1$ and $\mathbf{H}_2$, and the matrix $\mathbf{L}$ can be divided into four sub-matrix $\mathbf{L}_{11}, \mathbf{L}_{12}, \mathbf{L}_{21}$ and $\mathbf{L}_{22}$. Notice that in the steady state, the net flux is zero for all the nodes except the two source nodes. Thus, we have

$$\begin{pmatrix}\mathbf{L}_{11} & \mathbf{L}_{12}\\ \mathbf{L}_{21} & \mathbf{L}_{22}\end{pmatrix}\begin{pmatrix}\mathbf{H}_1\\ \mathbf{H}_2\end{pmatrix} = \begin{pmatrix}\mathbf{f}\\ 0\end{pmatrix}, \tag{13}$$

where $\mathbf{f} = (J_0, -J_0)^T$ with J_0 being the outgoing flux at the source T_h. For a given network topology and chosen i_0 and j_0, all the quantities in Eq. (13) are known, except $\mathbf{H}_2$ and $\mathbf{f}$. By $\mathbf{L}_{21}\mathbf{H}_1 + \mathbf{L}_{22}\mathbf{H}_2 = 0$ we have a unique nonzero solution $\mathbf{H}_2$. Substituting it into $\mathbf{L}_{11}\mathbf{H}_1 + \mathbf{L}_{12}\mathbf{H}_2 = \mathbf{f}$ we can obtain

f. That is, both $\mathbf{H}_2$ and **f** can be analytically solved. As **L** contains all the information of network topology, $\mathbf{H}_2$ and **f** will be seriously influenced by the network.

To confirm the theoretical derivation, we take the network correspond to Fig. 4(a) as an example. Firstly, we calculate the theoretical temperature distribution by Eq. (13), see the "stars" in Fig. 6, where the same results given twice in (a) and (b) are for clear comparison with the different simulation results. Then, we present the temperature distributions of simulation results for two specific cases of $n_0 = 0$ (without atoms on links) and $n_0 = 7$ (with 7 atoms on each link), respectively, as shown in Fig. 6, where "i" of x-axis represents the serial number of the node, the "T_i" of y-axis represents the temperature of the corresponding node, the "black solid circles" in Fig. 6 (a) is for the case of $n_0 = 7$, and "blue open circles" in Fig. 6 (b) is for the case of $n_0 = 0$. Comparing the two simulation results with the theoretical result in Fig. 6 (a) and (b), we can see clearly that the case of $n_0 = 7$ is much closer to the theoretical result than that of $n_0 = 0$ not only by the distance but also by the correlation, i.e. the case of $n_0 = 7$ is phase synchronized with the theoretical result. It should be emphasized here that the theoretical result is obtained by Eq. (13) under the situation of ignoring the interfacial thermal resistance, but in fact it exists in numerical simulation [9]. These results not only explain for the inconsistency between the case of $n_0 = 0$ and the theoretical result, but also indicates the phase synchronization comes from the only reasonable explanation that the added atoms on links can significantly reduce the effect of interface thermal resistances at nodes and thus lead to the *abnormal size effect*. This finding shows that the heat conduction in physical network is more complicated than our intuition, but the influence of network topology can be still traced.

5 Discussions and conclusions

In summary, we have presented a multi-body vibration model to study heat conduction in complex networks, and numerically find that their main heat fluxes are always localized in a subset for a variety of complex network topologies, indicating a localization phenomenon of heat conduction. To understand its mechanism, we introduce a transmission diagram to clearly show the distribution of heat fluxes on complex networks. Then, we investigate the different roles of the links in complex networks by removing them one by one, and surprisingly discovery a skeleton network. Further more, we find that there is a phase transition where the total heat flux of network has no obvious change when those links out of the skeleton are gradually removed but a larger change when the the links in the skeleton are removed. More importantly, by regulating the coupling strength between atoms inside and outside the skeleton, we confirm that the part inside the skeleton can promote the heat conduction in the network, while the part outside the skeleton can weaken the heat conduction in the network. In this sense, maybe we can make the heat fluxes of networks be pumped into the skeleton from outside the skeleton by the way of regulating the parameters of links inside the skeleton subnetwork, thus form a new type of thermal concentrator [37,38], implying potential applications in thermal management and thermal metamaterials. After that, we study the influence of link length and surprisingly find an abnormal size effect of heat conduction where the total heat flux of network can be enlarged with the increase of link length, in contrast to the previous results on 1D chains. Moreover, a brief theory referring to interface thermal resistances is introduced to explain the abnormal size effect. These findings may have potential applications in the aspects of optimizing integration methods for nanotubes/nanowires and thermal management in nano-networks etc.

Acknowledgements This work was partially supported by the National Natural Science Foundation of China under Grant Nos. 12005166, 11675056 and 11835003, and the Natural Science Foundation of Shaanxi Provincial Department of Education under Grant No. 20JK0764.

Competing Interests The Authors have declared that no competing interests exist.

References

1. Albert, R., Barabasi, A.: Statistical mechanics of complex networks. *Rev. Mod. Phys.* **74**, 47 (2002).
2. Boccaletti, S., Latora, V., Moreno, Y., Chavez, M., Hwang, D.-U.: Complex networks: Structure and dynamics. *Phys. Rep.* **424**, 175 (2006).
3. Dorogovtsev, S. N., Goltsev, A. V., Mendes, J. F. F.: Critical phenomena in complex networks. *Rev. Mod. Pyhs.* **80**, 1275 (2008).
4. Albert, R., Jeong, H., Barab¢si, A. L.: Error and attack tolerance of complex networks. *Nature* **406**, 378-382 (2000).
5. Stam, C. J.: Characterization of anatomical and functional connectivity in the brain: a complex networks perspective. *Int. J. Psychophysiology.* **77**, 186-194 (2010).
6. Pastor-Satorras, R., Castellano, C., Van Mieghem, P., Vespignani, A.: Epidemic processes in complex networks. Rev. Mod. Phys. **87**, 925 (2015).
7. Tian, C., Cao, L., Bi, H., Xu, K., Liu, Z.: Chimera states in neuronal networks with time delay and electromagnetic induction. Nonlinear Dynam. **93**, 1695-1704 (2018).
8. Wu, J., Zheng, M., Xu, K., Gu, C.: Effects of two channels on explosive information spreading. Nonlinear Dynam. **99**, 2387-2397 (2020).
9. Liu, Z. H., Wu, X., Yang, H. J., Gupte, N., Li, B. W.: Heat flux distribution and rectification of complex networks. New J. Phys. **12**, 023016 (2010).
10. Volkov, A. N., Zhigilei, L. V.: Scaling laws and mesoscopic modeling of thermal conductivity in carbon nanotube materials. Phys. Rev. Lett. **104**, 215902 (2010).
11. Xiong, K., Zhou, J., Tang, M., Zeng, C., Liu, Z.: Control of thermal conduction and rectification in a model of complex networks with two asymmetric parts. Phys. Rev. E **98**, 062144 (2018).
12. Xiong, K., Zeng, C., Liu, Z.: Effect of degree correlation on the thermal transport in complex networks. Nonlinear Dynam. **94**, 3067 (2018).

13. Xiong, K., Zeng, C., Liu, Z., Li, B.: Influence of the degree of a complex network on heat conduction. Phys. Rev. E **98**, 022115 (2018).
14. Xiong, K., Liu, Z., Zeng, C., Li, B.: Thermal-siphon phenomenon and thermal/electric conduction in complex networks. Natl. Sci. Rev. **7**, 270-277 (2020).
15. Xiong, K., Yan, Z., Xie, Y., Liu, Z.: Regulating heat conduction of complex networks by distributed nodes masses. Sci. Rep. **11**, 5501 (2021).
16. Lee, B. Y., Sung, M. G., Lee, H., Namgung, S., Park, S. Y., Choi, D. S., Hong, S.: Integrated devices based on networks of nanotubes and nanowires. NPG Asia. Mater. **2**, 103-111 (2010).
17. Ceylan, H. *et al*: Size-controlled conformal nanofabrication of biotemplated three-dimensional tio 2 and zno nanonetworks. Sci. Rep. **3**, 2306 (2013).
18. Yang, Y., Yang, X., Liang, L., Gao, Y., Cheng, H., Li, X., ..., Duan, X.: Large-area graphene-nanomesh/carbon-nanotube hybrid membranes for ionic and molecular nanofiltration. Science **364**, 1057-1062 (2019).
19. Pomerantseva, E., Bonaccorso, F., Feng, X., Cui, Y., Gogotsi, Y.: Energy storage: The future enabled by nanomaterials. Science **366**, 6468 (2019).
20. Son, D., Kang, J., Vardoulis, O., Kim, Y., Matsuhisa, N., Oh, J. Y., ..., Bao, Z.: An integrated self-healable electronic skin system fabricated via dynamic reconstruction of a nanostructured conducting network. Nat. nanotechnol. **13**, 1057-1065 (2018).
21. Kang, T. H., Chang, H., Choi, D., Kim, S., Moon, J., Lim, J. A., ..., Yi, H.: Hydrogel-templated transfer-printing of conductive nanonetworks for wearable sensors on topographic flexible substrates. Nano Lett. **19**, 3684-3691 (2019).
22. Hochstetter, J., Zhu, R., Loeffler, A., Diaz-Alvarez, A., Nakayama, T., Kuncic, Z.: Avalanches and edge-of-chaos learning in neuromorphic nanowire networks. Nat. Commun. **12**, 1-13 (2021).
23. Shen, D., Zhan, Z., Liu, Z., Cao, Y., Zhou, L., Liu, Y., ..., Yu, J.: Enhanced thermal conductivity of epoxy composites filled with silicon carbide nanowires. Sci. Rep. **7**, 1-11 (2017).
24. Vignolini, S., Yufa, N. A., Cunha, P. S., Guldin, S., Rushkin, I., Stefik, M., ..., Steiner, U.: A 3d optical metamaterial made by self-assembly. Adv. Mater. **24**, OP23-OP27 (2012).
25. Rauber, M., Alber, I., Muller, S., Neumann, R., Picht, O., Roth, C., ..., Ensinger, W.: Highly-ordered supportless three-dimensional nanowire networks with tunable complexity and interwire connectivity for device integration. Nano Lett. **11**, 2304-2310 (2011).
26. Lepri, S., Livi, R., Politi, A.: Thermal conduction in classical low-dimensional lattices. Phys. Rep. **377**, 1 (2003).
27. Dhar, A.: Heat transport in low-dimensional systems. Adv. Phys. **57**, 457 (2008).
28. Li, N., Ren, J., Wang, L., Zhang, G., Hanggi, P., Li, B.: Colloquium: Phononics: Manipulating heat flow with electronic analogs and beyond. Rev. Mod. Phys. **84**, 1045 (2012).
29. Liu, Z., Li, B.: Heat conduction in simple networks: The effect of interchain coupling. Phys. Rev. E **76**, 051118 (2007).
30. Lepri, S., Livi, R., Politi, A.: Heat conduction in chains of nonlinear oscillators. Phys. Rev. Lett. **78**, 1896 (1997).
31. Chen, J., Zhang, G., Li, B.: Molecular dynamics simulations of heat conduction in nanostructures: effect of heat bath. J. Phys. Soc. Jpn. **79**, 074604 (2010).
32. Hu, B., Li, B., Zhao, H.: Heat conduction in one-dimensional chains. Phys. Rev. E **57**, 2992 (1998).
33. Hu, B., Li, B., Zhao, H.: Heat conduction in one-dimensional nonintegrable systems. Phys. Rev. E **61**, 3828 (2000).
34. Li, B., Wang, L., Casati, G.: Thermal diode: Rectification of heat flux. Phys. Rev. Lett. **93**, 184301 (2004).
35. Kryven, I.: Bond percolation in coloured and multiplex networks. Nat Commun. **10**, 404 (2019).
36. Zhang, Y., Blattner, M., Yu, Y.: Heat conduction process on community networks as a recommendation model. Phys. Rev. Lett. **99**, 154301 (2007).
37. Shen, X., Li, Y., Jiang, C., Ni, Y., Huang, J.: A thermal theory for unifying and designing transparency, concentrating and cloaking. Appl. Phys. Lett. **109**, 031907 (2016).
38. Wang, R., Xu, L., Ji, Q., Huang, J.: J. Thermal cloak-concentrator. Appl. Phys. **123**, 115117 (2018).